ADMET & DMPK 13(5) (2025) 2961; doi: https://doi.org/10.5599/admet.2961

ADMET

Open Access : ISSN : 1848-7718

http://www.pub.iapchem.org/ojs/index.pH-p/admet/index

Original scientific paper

Elucidating CYP2D6-driven metabolism and hepatotoxic bioactivation of metoprolol in plateable human and animal hepatocytes

Jiang Pu, Mei Yang, Min Zhang, Ruiqi Gao, Yue Xiao, Lingyu Liu, Chuanjing Zhang, Wennuo Xu, Kaifang Li and Wanyong Feng*

Bioduro Biologics Co., Ltd., Shanghai, China

*Corresponding Author: E-mail: wanyong.feng@bioduro.com; Tel.: +86-021-31751005

Received: August 17, 2025; Revised: October 21, 2025; Published: October 30, 2025

Abstract

Background and purpose: As a classic β-blocker with low systemic clearance, metoprolol has been linked to rare but clinically significant hepatotoxicity, yet its hepatic metabolic fate remains poorly characterized. **Experimental approach:** Metoprolol was incubated individually in plateable human and animal hepatocytes, and recombinant cytochrome *(*CYP) P450 enzymes, followed by sample processing for cytotoxicity assessment, stability analysis, phenotyping and metabolite identification studies. **Key results:** *In vitro* cytotoxicity assessment revealed distinct species-specific responses to metoprolol exposure. Metoprolol showed no observable cytotoxicity across the tested concentration range (0 to 500 μM) in human hepatocytes, whereas it was cytotoxic only at a concentration of 500 μM in rat hepatocytes. Metabolic characterization showed low intrinsic clearance in human hepatocytes (0.56±0.12 μL min^{-1} *per* million cells) over a 72-hour incubation. Comprehensive mass spectrometer analysis identified 22 metabolites across four species (rat, dog, monkey, and human) and fifteen metabolites were identified as the new ones, with CYP2D6-mediated biotransformation pathways (including mono-oxygenation, *O*-demethylation, and oxidation) accounting for the generation of four major metabolites (M1, M10, M13, M17). Notably, species-specific metabolism was observed for α-hydroxy-metoprolol (M10). It served as the predominant metabolite in rat hepatocytes and underwent subsequent bioactivation to a reactive glutathione (GSH) conjugate. Inhibition studies with 1-aminobenzotriazole (a non-specific CYP inhibitor) confirmed the CYP-dependent nature of this hepatotoxic metabolic pathway. **Conclusion**: The sustained metabolic activity of plateable hepatocytes facilitated a comprehensive metabolic profiling of metoprolol, including direct observation of GSH-mediated bioactivation. Integrating with cytotoxicity data, these findings offered crucial insights into its hepatic adverse effects.

Keywords

Metabolite; cytotoxicity; recombinant; low-clearance; glutathione; CYP2D6

Introduction

Hepatic metabolism is the primary pathway for clearing xenobiotic compounds from the body. Approximately 70 % of marketed pharmaceuticals are metabolized in the liver through its detoxification functions [1,2]. It is well established that high hepatic clearance often results in low systemic bioavailability. Conversely, a detailed understanding of hepatic metabolism can support drug optimization efforts by revealing metabolic soft spots in lead compounds [3]. Consequently, hepatocytes play an indispensable role in drug discovery.

Hepatocytes are the preferred *in vitro* model for metabolism studies due to their complete complement of phase I and II enzymes, which accurately recapitulate intrinsic clearance mechanisms [4-13]. These cells also express the full spectrum of hepatic transporters that govern drug uptake and efflux, providing a physiologically relevant platform for disposition studies [14,15]. Notably, comparative metabolite profiling across species-specific hepatocytes enables prediction of interspecies metabolic differences, thereby informing appropriate animal model selection for preclinical toxicology assessments [16,17].

Recent years have witnessed notable advancements in hepatocyte systems for low-clearance compound assessment, including suspended hepatocytes and adherent primary hepatocytes, HepaRG cells [18-25], and various hepatocyte-stromal cell cocultures [26-47]. Adherent primary hepatocytes are optimal for low-clearance compound studies due to their stable metabolic function and intact enzyme systems in extended cultures. Traditional hepatocellular carcinoma cell lines are limited by genetic instability and progressive phenotypic drift, and coculture systems present operational challenges due to the biological complexity imposed by heterologous cellular components. Although suspended hepatocytes are commonly used for metabolic screening, their utility is severely hampered by the rapid loss of enzymatic activity within 4 hours [25,42,48]. Methods like the relay technique [24] extend observation periods via sequential incubations but complicate routine application [42,49]. In contrast, adherent primary hepatocytes maintain robust metabolic enzyme activity and intact hepatic enzymatic profiles without artificial modification, rendering them the most physiologically relevant *in vitro* model for prolonged clearance studies [50-52]. Compelling evidence from Griffin *et al.* [53] demonstrated superior performance of plateable rat hepatocytes compared to suspended cells for low-clearance measurements. Subsequent human hepatocyte studies have validated the reliability of adherent systems for evaluating low-clearance compounds [20,54].

Despite being extensively utilized as both a CYP2D6 phenotyping probe and a model high-permeability compound exhibiting excellent oral bioavailability [55-59], metoprolol's complete metabolic disposition as a low-clearance agent [60,61] remains insufficiently characterized, particularly regarding its hepatic elimination pathways. Existing metabolite identification studies are conducted in various matrices, including rat plasma [62,63], human liver microsomes, plasma, and urine [57,64-68], as well as dog plasma [69]. Only minor metabolites are reported *in vivo*, a fact attributed to the significant renal excretion. Moreover, even fewer metabolites are typically observed *in vitro* under short-term incubation conditions. This study, therefore, aims to systematically characterize metoprolol metabolism using plateable hepatocytes with longer extended culture and recombinant enzymes, providing novel insights into its hepatic adverse effects.

Experimental

Chemicals and reagents

Metoprolol (CAS: 51384-51-1, Lot: 6-JKL-52-4) was purchased from TRC Canada, while α-hydroxy-metoprolol (CAS: 56392-16-6, Lot: H2429287) and metoprolol acid (CAS: 56392-14-4, Lot: L2213483) were obtained from Aladdin. Hepatocytes from male Sprague-Dawley rats (HEP134054, 10 donors), male Beagle dogs (CDH100BE-V11201, 1 donor), male Cynomolgus monkeys (23D008, 1 donor), and male Caucasians (005, 1 donor) were sourced from Biopredict, TPCS, IPHASE, and XENOTECH, respectively. The kit of CellTiter-Glo® Luminescent Cell Viability Assay (Lot#: 0000582333) was purchased from Promega. Recombinant enzymes, including CYP1A2 (Lot#: C1A2R015A), CYP2D6 (Lot#: C2D6R040), CYP2C9 (Lot#: C2C9BR014), CYP2C19 (Lot#: C2C19BR027), CYP3A4 (Lot#: C3A4BR054), CYP2B6 (Lot#: C2B6BR057), and CYP2C8 (Lot#: C2C8BR008A), were acquired from Cypex for enzymatic activity studies. 48-well (Lot#: 11520012) and 96-well (Lot#: 31219012) Collagen I-pre-coated plates were purchased from Corning.

Plateable hepatocytes cytotoxicity

Cryopreserved plateable rat and human hepatocytes were thawed by immersing vials in a pre-warmed 37 °C water bath. The cell pellets were then transferred to thawing medium and centrifuged to isolate viable cells. Then, hepatocytes were diluted to 0.1 million cells mL^{-1} and seeded into 96-well plates (0.1 mL *per* well) in triplicate. After 6 hours of attachment, the plating medium was replaced with incubation medium containing 1 % Matrigel™. On the following day, the cell medium was replaced with a series of metoprolol dosing solutions (0, 100, 150, 200, 250 and 500 µM) in the presence or absence of 50 µM 1-aminobenzotriazole (ABT), a cytochrome P450 inhibitor, and then the hepatocyte cytotoxicity was determined using a commercially available ATP detection assay (CellTiter-Glo®). Prior to the measurement, the cell culture plate was equilibrated to ambient temperature. Subsequently, 100 µL of CellTiter-Glo® reagent was dispensed into each well, followed by orbital shaking (5 min) to ensure complete cell lysis. After a 10-minute stabilization at room temperature, luminescence signals were quantified using an envision® multilabel plate reader.

Plateable hepatocytes stability

Cryopreserved human hepatocytes were thawed by immersing vials in a pre-warmed 37 °C water bath. The cell pellets were then transferred to thawing medium and centrifuged to isolate viable cells. Then, hepatocytes were diluted to 0.7 million cells mL^{-1} and seeded into collagen-coated 48-well plates (0.2 mL *per* well) in triplicate. After 6 hours of attachment, the plating medium was replaced with incubation medium containing 1 % Matrigel™. On the following day, the medium was replaced with a dosing solution containing 1 µM metoprolol to initiate metabolic reactions. Aliquots were collected at 0, 2, 4, 8, 24, 48 and 72 hours, and reactions were quenched with cold acetonitrile/methanol (1:1, v/v) containing labetalol (100 ng mL^{-1}). After centrifugation (12,000*g*, 15 min, 4 °C), supernatants were analysed *via* LC-30AD-API5500 (LC-MS/MS, SCIEX, USA) for semiquantitative assessment.

Recombinant cytochrome P450 reaction phenotyping

Human recombinant enzymes were diluted to 50 pmol mL^{-1} in 50 mM phosphate buffer. Metoprolol was added to the enzyme solution (final concentration: 1 µM) in duplicate and preincubated for 5 min. Reactions were initiated by adding NADPH (final concentration: 1 mM) and aliquots were collected at 0, 15, 30, 60 and 120 min. Samples were quenched with cold acetonitrile containing tolbutamide (10 ng/mL), centrifuged (12,000*g*, 15 min, 4 °C) and analysed by LC-MS/MS. For qualitative metabolite analysis, 0- and 60-minute samples were dried, reconstituted, centrifuged (12,000*g*, 15 min, 4 °C) and analysed on Ultimate 3000-Q-Exactive Plus (LC-HRMS, ThermoFisher, Germany).

Metabolite identification in recombinant cytochrome 2D6 enzymes and plateable hepatocytes

Human recombinant cytochrome 2D6 enzymes were diluted to 50 pmol mL^{-1} in 50 mM phosphate buffer. Metoprolol was added to the enzyme solution (final concentration: 1 µM) in duplicate and preincubated for 5 min. Reactions were initiated by adding NADPH (final concentration: 1 mM), and aliquots were collected at 60 min. Samples were quenched with cold acetonitrile containing 0.1 % formic acid, centrifuged (12,000*g*, 15 min, 4 °C), then supernatants were dried, reconstituted, centrifuged (12,000*g*, 15 min, 4 °C), and subjected to an analysis on LC-HRMS..

Cryopreserved rat, dog, monkey and human hepatocytes were thawed by immersing vials in a pre-warmed 37 °C water bath. The cell pellets were then transferred to thawing medium and centrifuged to isolate viable cells. Then, hepatocytes were diluted to 0.7 million cells mL^{-1} and seeded into collagen-coated 48-well plates (0.2 mL *per* well) in duplicate. After 6 hours of attachment, the plating medium was replaced

with incubation medium containing 1 % Matrigel™. On the following day, the medium was replaced with a dosing solution containing 10 µM metoprolol to initiate metabolic reactions. Reactions were quenched at 72 hours with cold acetonitrile containing 0.1 % formic acid, and supernatants were dried under nitrogen gas. The residues were reconstituted in acetonitrile/water (1:9 volume ratio) with 0.1 % formic acid and analysed LC-HRMS. The M7 metabolite was isolated, purified, and concentrated via a mass spectrometry switching valve, followed by sample reconstitution, and subsequent analysis on LC-HRMS.

Semi-quantitative and qualitative analysis

Semi-quantitative LC-MS/MS analysis was performed using an LC30 pump (Shimadzu, Japan) coupled to an API 5500 mass spectrometer. The mobile phase A was distilled water containing 0.1 % formic acid and the mobile phase B was acetonitrile containing 0.1 % formic acid. The LC gradient was as follows: 0 to 0.80 min at 5 % B; 0.80 to 1.20 min, 5 to 95 % B; 1.20 to 1.80 min at 95 % B; 1.80 to 1.81 min, 95 to 5 % B; and 1.81 to 2.5 min at 5 % B (flow rate: 0.8 mL min^{-1}). MS parameters included: curtain gas: 2.76 MPa, gas 1: 2.76 MPa, gas 2: 4.14 MPa, ion source voltage: 5500 V, source temperature: 550 °C, auxiliary nitrogen pressure: 0.7 MPa, and entrance potential voltage: 10 eV. Data was acquired in multiple ions monitor mode using Analyst 1.6.3 software (SCIEX, USA; https://sciex.com/products/software/analyst-software).

Qualitative LC-HRMS analysis was conducted using an Ultimate 3000 pump (ThermoFisher, Germany) and a Q-Exactive Plus spectrometer. The mobile phase A was distilled water containing 0.1 % formic acid and the mobile phase B was acetonitrile containing 0.1 % formic acid. The liquid chromatography (LC) gradient spanned 22 min: 0 to 1.0 minute at 5 % B; 1.0 to 6.0 min, 5 to 15 % B; 6.0 to 14.0 mi, 15 to 25 % B; 14.0 to 16.0 min, 25 to 90 % B; 16.0 to 18.0 min, 90 to 95 % B; 18.0 to 20.0 min, 95 to 5 % B; and 20.0 to 22.0 min at 5 % B (flow rate: 0.3 mL min^{-1}). MS parameters included: spray voltage: 3.8 kV, capillary temperature: 320 °C, heater temperatures: 350 °C, sheath gas: 2.76 MPa, auxiliary nitrogen pressures: 0.7 MPa and tube lens voltage: 10 eV. The full scan Q1 resolution was set to 70,000, and the automatic gain control (AGC) target value was set to 5×10^5 intensity. The maximum injection time was limited to 50 ms. The dd-MS^2 resolution was set at 17,500, with the AGC target set at 5×10^4. External calibration was performed, yielding a deviation of less than 5.0 *ppm*. Data was processed using Xcalibur 4.1.31.9 software (ThermoFisher, Germany; https://www.thermofisher.com/order/catalog/product/OPTON-30965).

Data analysis

LC-MS/MS raw data was analysed using Analyst software, and hepatic clearance results (mean±SD) was processsed with GraphPad Prism 5.0 (GraphPad software, USA; https://www.graphpad.com/). Phenotyping data (mean values) was analysed using Microsoft Excel 2021 (mean values). Hepatic clearance was determined by quantifying metoprolol depletion following incubation with hepatocytes. The *in vivo* hepatic clearance was subsequently extrapolated using the well-stirred model incorporating intrinsic clearance [70-72]. Hepatocyte viability data was expressed as mean±SD. The statistical significance was determined by Student's *t*-test using GraphPad Prism. LC-HRMS raw data was extracted with Xcalibur, and metabolites were identified using Compound Discoverer 3.0 (ThermoFisher, Germany; https://www.thermofisher.com/order/catalog/product/OPTON-31061) by comparing fragment patterns between parent compounds, metabolites, and standards.

Results and discussion

Hepatocytes viability, metabolic stability and phenotyping study

The cytotoxic effects of metoprolol were assessed in plateable rat and human hepatocytes using the CellTiter-Glo® Luminescent Cell Viability Assay. In rat hepatocytes, metoprolol exhibited weak cytotoxicity,

with significant reductions (>30 %) in cell viability observed at 500 µM (Figure 1a). 1-Aminobenzotriazole was a classic inhibitor of CYP450 enzymes; pre-treatment with ABT significantly increased the viability of rat hepatocytes and reversed the cytotoxic effect at 500 µM. In contrast, human hepatocytes demonstrated greater resistance to metoprolol-induced cytotoxicity (Figure 1b). No significant reduction in cell viability was observed across the tested concentration range (0 to 500 µM), regardless of ABT co-treatment.

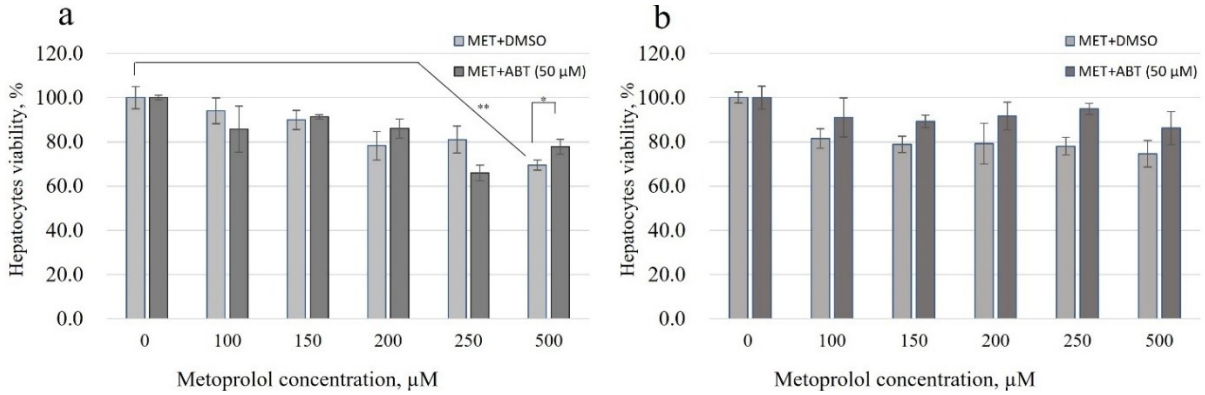

Figure 1. (a) rat and (b) human hepatocytes viability after 48 hours of treatment with metoprolol with or without the presence of ABT. *p < 0.05, **p < 0.01

These metabolic stability studies demonstrated that metoprolol exhibited typical low-clearance characteristics in plateable hepatocytes, with an *in vitro* intrinsic clearance (CL_{int}) of 0.56±0.12 µL min^{-1} *per* million cells (Figure 2a) and a corresponding *in vivo* CL_{int} of 1.59±0.31 mL min^{-1} kg^{-1}. These values are significantly below the 10 mL min^{-1} kg^{-1} threshold for low-clearance compounds and align well with previously reported [20,54] with a low clearance of 2.2 ± 0.7 µL min^{-1} *per* million cells in plateable human hepatocytes, correlating with an *in vivo* clearance of 1.4 mL min^{-1} kg^{-1} [20] (or 4.28 µL min^{-1} *per* million cells [73]), making the plateable hepatocytes particularly valuable for evaluating low-clearance compounds [74].

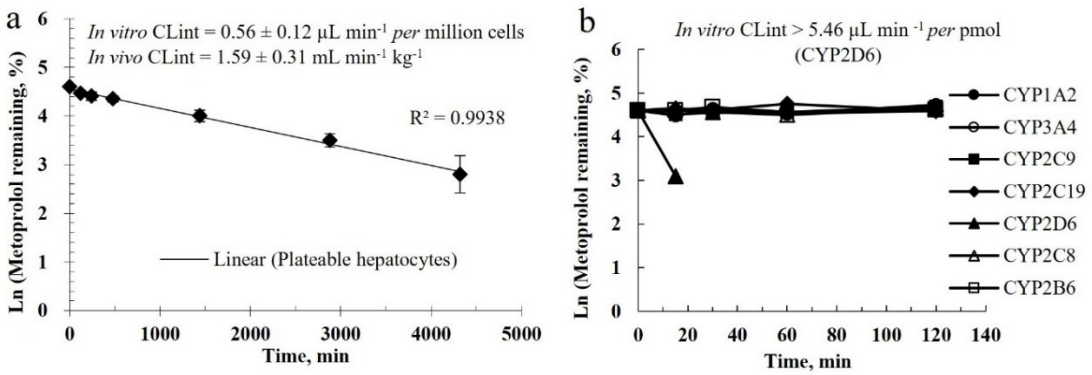

Figure 2. Metoprolol Remaining *vs.* incubation time in (a) plateable hepatocytes and (b)recombinant enzymes

Enzyme phenotyping studies demonstrated remarkable specificity in metoprolol metabolism. As illustrated in Figure 2b, among the cytochrome P450 isoforms tested (CYP1A2, 2C9, 2C19, 3A4, 2B6 and 2C8), only CYP2D6 displayed significant metabolic activity, contributing to 100 % of the observed clearance with an intrinsic clearance rate of 5.46 µL min^{-1} *per* pmol protein. This finding corroborates prior reports on the exclusive involvement of CYP2D6 in metoprolol metabolism [58], highlighting its critical clinical implications. Given this highly selective CYP2D6-dependent metabolic pathway, these results emphasize the importance of genotype-guided dosing strategies, particularly in populations with a high prevalence of CYP2D6 poor metabolizers.

Chromatographic and mass spectrometric characteristics of metoprolol and its metabolites

In Figure 3, metoprolol was determined with a protonated molecular ion peak at *m/z* 268.1914. The collision-induced dissociation (CID) product ion spectrum exhibited characteristic fragment ions at *m/z* 56.0499,

72.0810, 98.0967, 116.1073, 121.0652, 133.0652, 159.0811 and 191.1075, supporting its structural identification. The LC analysis showed a retention time of approximately 10.86 min for the parent compound.

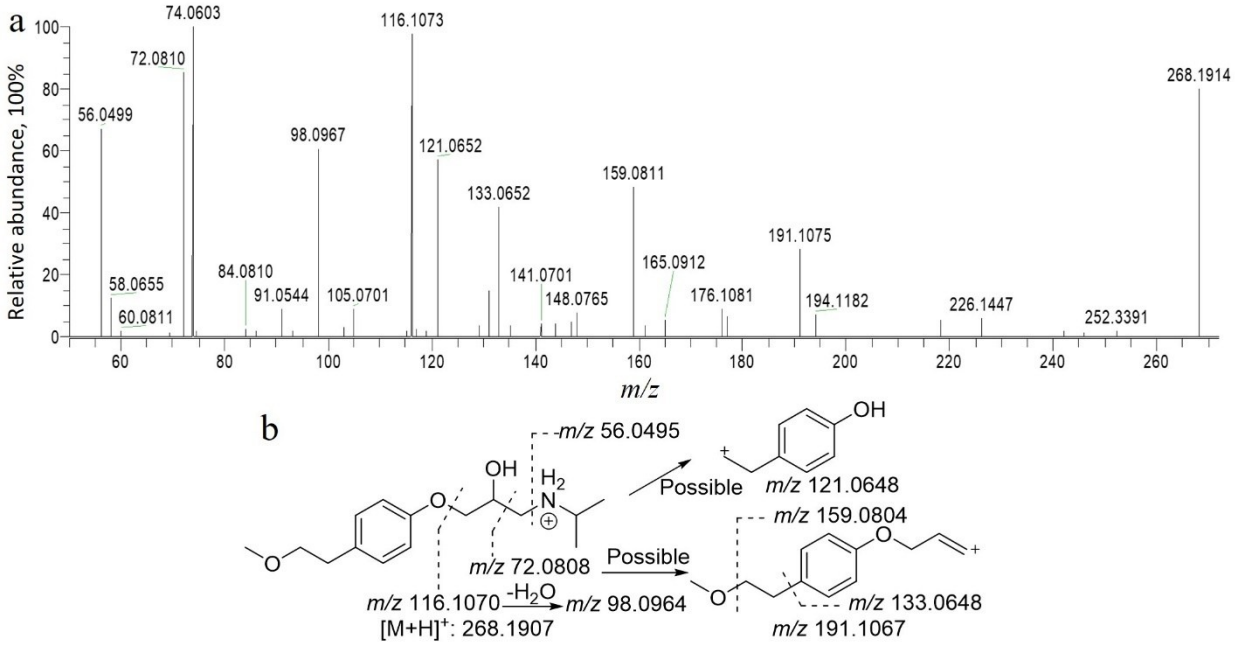

Figure 3. Collision-induced dissociation spectrum (**a**) and structural analysis (**b**) of metoprolol

As summarized in Table 1 and illustrated in Figure 4, twenty-two metabolites were detected and fifteen were identified as new in plateable hepatocytes, eluting between 2.64 and 13.52 min, with effective chromatographic separation. Species-dependent metabolic profiles were observed in the metabolite identification results in plateable hepatocytes.

Table 1. Observed metabolites of metoprolol in recombinant 2D6 enzymes and plateable hepatocytes

ID	RT, min	*m/z* (+)		ME, *ppm*	Metabolic pathway	Relative peak area, %					Ref.
		Theoretical	Detected			Plateable hepatocytes				2D6[a]	
						R	D	Mk	H	H	
M1	2.65	270.1700	270.1711	4.1	*O*-demethylation and mono-oxygenation	8.8	0.8	4.7	D	26.6	-
M2	2.72	284.1492	284.1503	3.9	Oxidation and mono-oxygenation	0.9	D	0.1	ND	ND	-
M3	3.65	212.1281	212.1288	3.3	*O*-demethylation and *N*-dealkylation	D	0.7	0.1	ND	1.6	-
M4	4.44	226.1074	226.1082	3.5	*N*-dealkylation and oxidation	D	ND	D	ND	ND	-
M5	5.08	268.1543	268.1552	3.4	*O*-demethylation, mono-oxygenation, and dehydrogenation	0.6	D	0.1	ND	2.0	-
M6	5.82	444.1864	444.1878	3.2	*O*-demethylation, mono-oxygenation, dehydrogenation and glucuronidation	0.1	ND	0.1	ND	ND	-
M7	5.86	589.2538	589.2511	-4.6	Mono-oxygenation and glutathionylation (displacement)	D	ND	ND	ND	ND	[63]
M8	5.96	270.1700	270.1713	4.8	*O*-demethylation and mono-oxygenation	0.1	ND	ND	ND	ND	-
M9	6.12	254.1387	254.1395	3.1	Oxidation	0.4	D	0.2	D	1.7	[69]
M10	6.42	284.1856	284.1863	2.5	Mono-oxygenation	24.4	9.4	5.6	2.7	20.1	[62,63, 66-69,73]
M11	6.57	430.2072	430.2085	3.0	*O*-demethylation and glucuronidation	0.1	D	0.2	ND	ND	-
M12	6.70	430.2072	430.2082	2.3	*O*-demethylation and glucuronidation	D	D	0.2	D	ND	-
M13	6.79	254.1751	254.1755	1.6	*O*-demethylation	3.8	20.5	0.1	6.0	22.8	[62,63, 66,69,73]

ID	RT, min	*m/z* (+)		ME, *ppm*	Metabolic pathway	Relative peak area, %					Ref.
		Theoretical	Detected			Plateable hepatocytes				2D6[a]	
						R	D	Mk	H	H	
M14	6.97	589.2538	589.2511	-4.6	Mono-oxygenation and glutathionylation (displacement)	D	ND	ND	D	ND	[63]
M15	7.19	444.1864	444.1875	2.5	*N*-dealkylation, acetylation and glucuronidation	D	ND	0.5	0.2	ND	-
M16	7.27	282.1700	282.1709	3.2	Mono-oxygenation and dehydrogenation	1.3	0.1	D	D	0.5	-
M17	7.36	268.1543	268.1551	3.0	Oxidation	57.2	19.9	82.6	14.6	18.3	[57]
M18	7.80	226.1438	226.1443	2.2	*N*-dealkylation	0.1	5.8	D	D	6.4	[69]
M19	10.16	444.2228	444.2236	1.8	Glucuronidation	D	D	4.2	0.7	ND	-
P	10.66	268.1907	268.1914	2.6		2.1	42.5	1.2	75.8	ND	-
M20	12.52	460.2177	460.2189	2.6	Mono-oxygenation and glucuronidation	ND	0.1	D	ND	ND	-
M21	13.05	258.1336	258.1340	1.5	*N*-dealkylation and di-oxygenation	0.1	0.2	D	D	ND	-
M22	13.52	460.2177	460.2189	2.6	Mono-oxygenation and glucuronidation	ND	D	0.1	ND	ND	-

ID - identity; RT – retention time; ME - mass error; 2D6[a] - recombinant 2D6 enzymes; D - detected in trace amount; ND - not detected; R -rat; D -dog; Mk - monkey; H - human. The relative peak area abundance of the parent and metabolite was calculated based on their selected ion chromatographic peak areas.

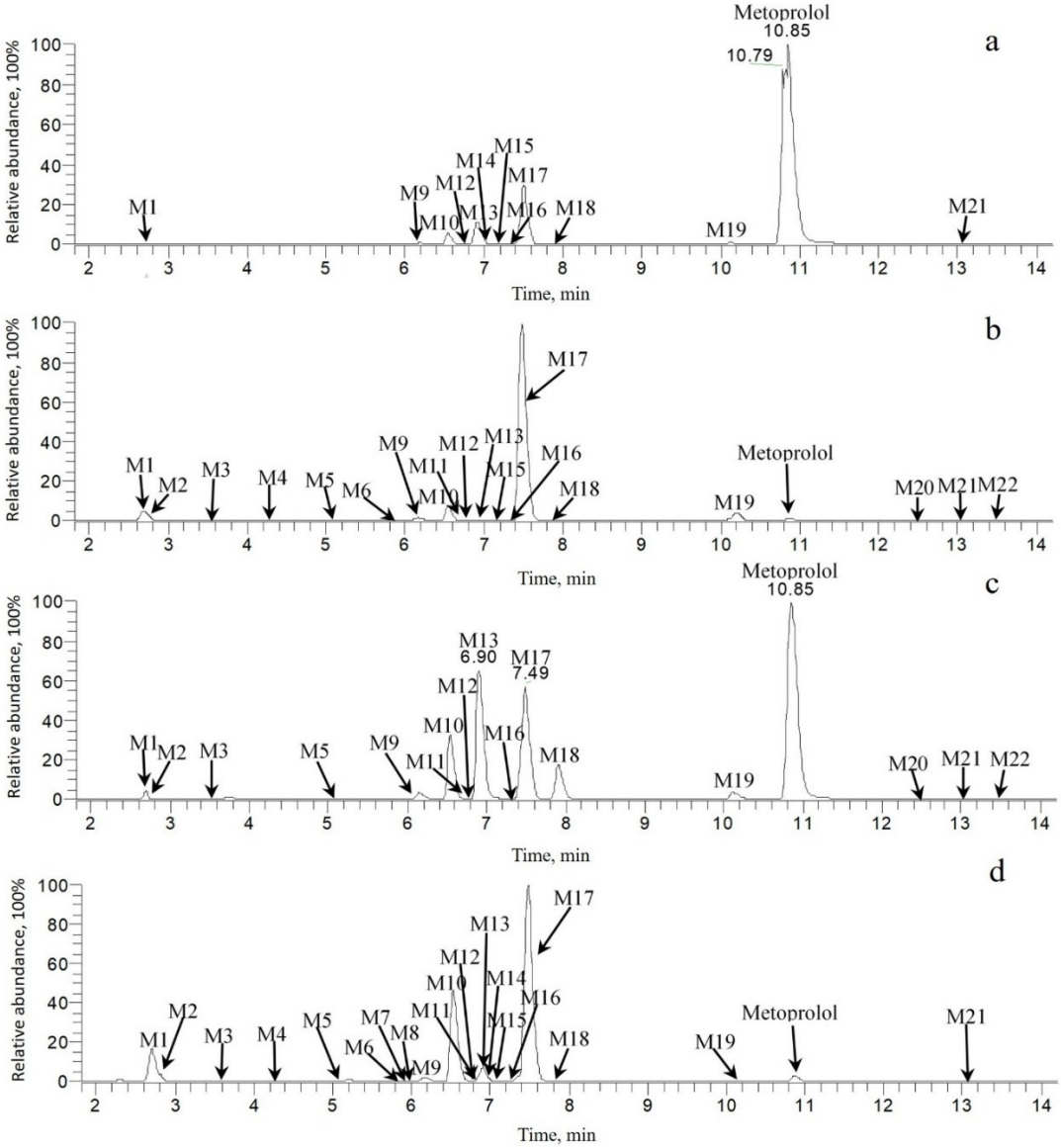

Figure 4. Selected ion chromatograms of metoprolol and its metabolites in plateable human (a), monkey (b), dog (c) and rat (d) hepatocytes

In rat hepatocytes, M10 and M17 predominated, constituting 24.4 and 57.2 % of the total mass abundance, respectively. In dog hepatocytes, M13 and M17 were the major metabolites, accounting for 20.5 and 19.9 %. Notably, in monkey and human hepatocytes, M17 was the dominant metabolite, representing 82.6 and 14.6 % of the total mass abundance, respectively. According to the metabolite identification result in recombinant CYP2D6 enzymes, the most abundant metabolites were M1, M10, M13, and M17, with relative abundances of 26.6, 20.1, 22.8 and 18.3 %, respectively. Across all tested species and matrices, the major metabolic pathways consisted of mono-oxygenation, *O*-demethylation, and oxidation, with CYP2D6 confirmed as the principal enzyme mediating these biotransformations as shown in Figure 5.

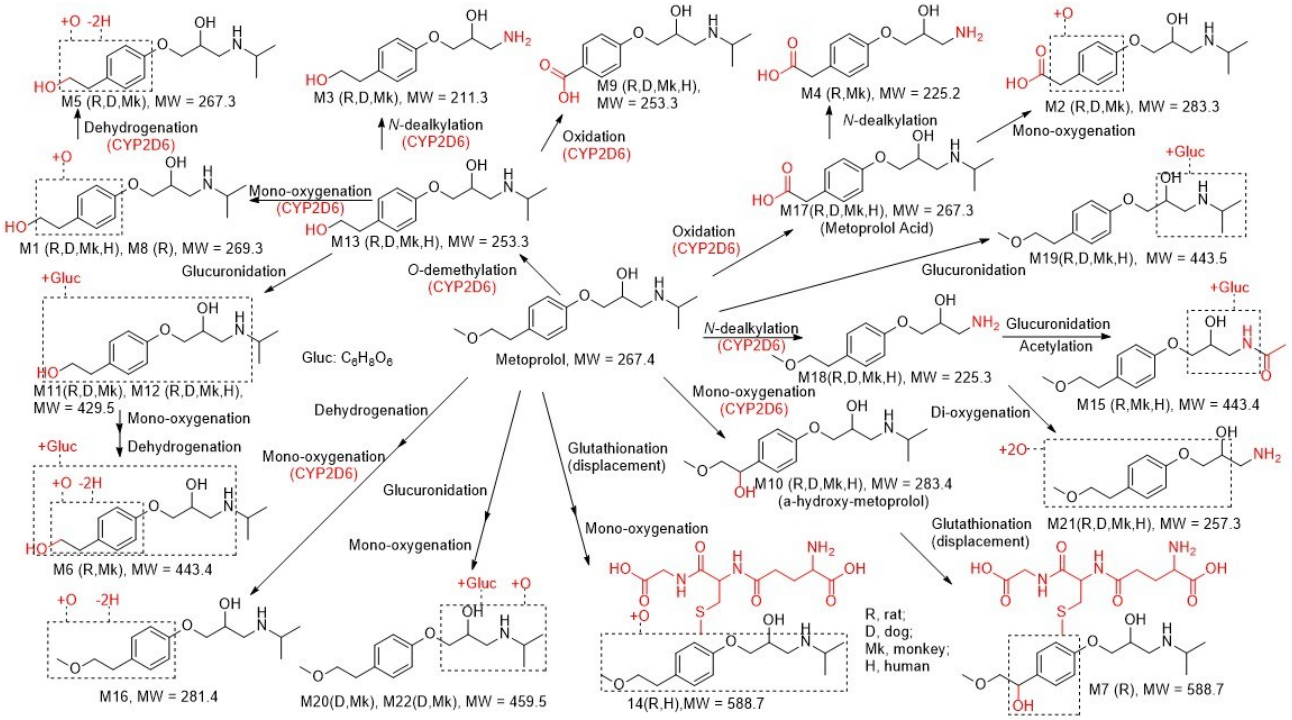

Figure 5. Proposed metabolic pathways of metoprolol in plated hepatocytes and CYP2D6 recombinant enzymes

Metabolites elucidation

Metabolite structures were deduced based on mass defect analysis and fragmentation patterns.

Oxygenation derivatives

M10 exhibited a protonated molecular ion at *m*/*z* 284.1863; its characteristic ions were observed at *m*/*z* 56.0500, 74.0603, 98.0968, 116.1074, and specifically at *m*/*z* 207.1025, indicating that M10 was a mono-oxygenation metabolite. M10 eluted at a retention time of 6.55 min, which was close to that of α-hydroxy-metoprolol. Furthermore, M10 and α-hydroxy-metoprolol shared similar fragment ions at *m*/*z* 74.0600, 98.0964, 116.1069, 133.0647 and 207.1015, suggesting they were closely related.

M16 exhibited a protonated molecular ion at *m*/*z* 282.1709, with characteristic ions at *m*/*z* 173.0601, 205.0869 and 240.1228, indicating that M16 was a metabolite of mono-oxygenation and dehydrogenation.

O-demethylation products

M13 exhibited a protonated molecular ion at *m*/*z* 254.1755, with characteristic ions at *m*/*z* 116.1072, 159.0808 and 177.0914, indicating that M13 was an *O*-demethylation metabolite.

M1 and M8 displayed the same protonated molecular ion at *m*/*z* 270.171, along with identical characteristic ions at *m*/*z* 175.0760 and 193.0866, suggesting a mono-oxygenation reaction on M13.

M3 presented a protonated molecular ion at *m/z* 212.1288, with characteristic ions at *m/z* 74.0603, 159.0810, and 177.0915. No modification was detected on the *m/z* 177.0915 moiety, and *N*-dealkylation was confirmed by the indirect fragment at *m/z* 74.0603, which was dealkylated from *m/z* 116.1072, therefore, M3 was classified as a metabolite of both *O*-demethylation and *N*-dealkylation.

M5 displayed a protonated molecular ion at *m/z* 268.1552, with characteristic ions at *m/z* 116.1074, 191.0708, and 226.1079. No modification was detected on the *m/z* 116.1074 moiety, while dehydrogenation was observed on the moieties at *m/z* 191.0708 and *m/z* 226.1079 compared to M1 or M8, therefore, M5 was identified as a dehydrogenation metabolite from M1 or M8.

Oxidative transformations

M9 exhibited a protonated molecular ion at *m/z* 254.1395, its characteristic ions were observed at *m/z* 116.1075, 151.0396, 133.0653, and 177.0553, indicating that M9 was an oxidation metabolite.

M17 exhibited a protonated molecular ion at *m/z* 268.1551, its characteristic ions were observed at *m/z* 116.1073, 145.0653, 191.0708, and 226.1082. A special transition of loss of carboxyl group from *m/z* 191.0708 to *m/z* 145.0653 suggested that M17 was an oxidation metabolite. Furthermore, M17 was eluted at a retention time of 7.52 min, which was close to that of metoprolol acid, and they shared similar fragments at *m/z* 56.0498, 98.0964, 116.1069, 145.0647, 191.0701, 226.1073, and 250.1437. Therefore, M17 was identified as metoprolol acid.

M2 displayed a protonated molecular ion at *m/z* 284.1503, with characteristic ions at *m/z* 116.1074, 189.0552, and 207.0659. No modifications occurred on the *m/z* 116.1074 moiety, suggesting that M2 was a mono-oxygenation metabolite originating from M17.

M4 exhibited a protonated molecular ion at *m/z* 226.1082, with characteristic ions at *m/z* 56.0499, 74.0603, 145.0652, and 191.0709. No modifications were observed on the *m/z* 191.0709 moiety, indicating that M4 was an *N*-dealkylation metabolite derived from M17.

N-dealkylation modifications

M18 exhibited a protonated molecular ion at *m/z* 226.1443, with characteristic ions at *m/z* 74.0603 and *m/z* 191.1072. No modifications were detected on the *m/z* 191.1072 moiety, and *N*-dealkylation was confirmed by a transition from *m/z* 116.1072 to *m/z* 74.0603. Therefore, M18 was identified as a metabolite resulting from *O*-demethylation and *N*-dealkylation.

M21 presented a protonated molecular ion at *m/z* 258.1340, with a characteristic ion at *m/z* 209.0814, indicating that M21 was a di-oxygenation metabolite of M18.

Glucuronide conjugates

M6 showed a protonated molecular ion at *m/z* 444.1878, with characteristic ions at *m/z* 116.1073, 226.1074, and 268.1547, indicating that M6 was a metabolite of *O*-demethylation, mono-oxygenation, dehydrogenation and glucuronidation.

M11 and M12 exhibited the same protonated molecular ion at *m/z* 430.208, along with a common characteristic ion at *m/z* 254.176, which showed a significant transition of glucuronidation loss; thus, they were identified as glucuronidation metabolites derived from M13.

M15 displayed a protonated molecular ion at *m/z* 444.1875, with characteristic ions at *m/z* 191.0709 and 268.1550. No modifications were observed on the *m/z* 191.1075 moiety, and a glucuronide loss (-176 amu) was detected from *m/z* 444.1875 to 268.1550. Consequently, M15 was characterized as a metabolite of

acetylation and glucuronidation derived from M18.

M19 displayed a protonated molecular ion at *m/z* 444.224, with characteristic ions at *m/z* 116.1073 and 268.1914. A notable glucuronide loss (-176 amu) was detected, transitioning from *m/z* 444.224 to 268.191, leading to its identification as a glucuronidation metabolite.

M20 and M22 displayed the same protonated molecular ion at *m/z* 460.219, and they exhibited identical characteristic ions at *m/z* 114.092 and 284.186, indicating that they were metabolites resulting from mono-oxygenation and glucuronidation.

Glutathione conjugates

M7 and M14 exhibited a common protonated molecular ion at *m/z* 295.1287 (*z* = 2). The characteristic ions observed were *m/z* 130.0498, 179.0483, 308.0923 and 282.1696. Considering these ions at *m/z* 130.0498, 179.0483 and 308.0923 were characteristic fragments of glutathione conjugates. Moreover, mass spectrometric analysis of the concentrated M7 metabolite showed enhanced glutathione-associated fragment peaks (Figure 6), providing evidence for potential glutathione adduct formation. Therefore, M7 and M14 were metabolites resulting from mono-oxygenation and glutathionylation (displacement).

Despite its classification as a low clearance drug, the comprehensive metabolic fate of metoprolol remains incompletely characterized in current literature. Notably, our study has identified up to 22 metabolites in plateable hepatocytes, as shown in Table 1, significantly expanding upon previously identified metabolites [62-69,75,76]. Tao *et al* [62] identified two metabolites, α-hydroxy-metoprolol (*m/z* 116.1, 133.1, 163.1 and 207.1) and *O*-desmethyl-metoprolol (*m/z* 98.1, 116.1, and 177.1). Both metabolites were also detected in plateable hepatocytes, with more abundant fragments for α-hydroxy-metoprolol (*m/z* 56.0500, 74.0603, 86.0966, 98.0968, 116.1074, 133.0653, 163.0758, 207.1025 and 224.1289) and *O*-desmethyl-metoprolol (*m/z* 56.0499, 72.0810, 74.0602, 98.0966, 116.1072, 133.0651, 151.0757, 159.0808, 177.0914 and 212.1285). Li *et al.* [63] and Bae *et al.* [67] reported the formation of reactive glutathione adducts through the artificial addition of the xenobiotic glutathione cofactor. Consistent with this, two glutathione adducts were directly captured in plateable rat and human hepatocytes, demonstrating prolonged metabolic enzyme activity.

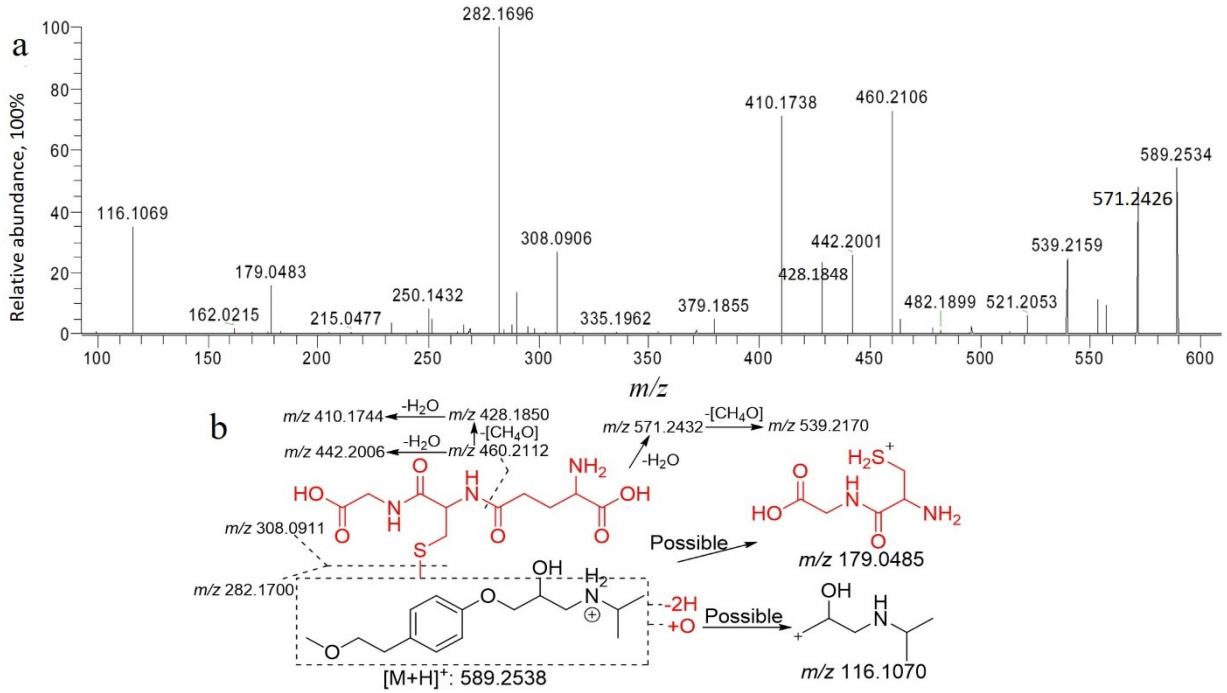

Figure 6. Collision-induced dissociation spectrum (a) and structural analysis (b) of M7

Aligning with the findings reported by Ma *et al.* [77], plateable hepatocytes effectively captured the low-clearance characteristics and pronounced interspecies differences in metoprolol metabolism after prolonged incubation. Human plateable hepatocytes maintained functional cytochrome P450 enzymes and accurately recapitulated metabolism mediated by human recombinant CYP2D6 enzymes, with principal metabolites exhibiting comparable relative abundance profiles (M10, M13, and M17). Notably, M10 was a minor metabolite in human plateable hepatocytes but constituted the major metabolite in rat plateable hepatocytes. Moreover, M10 demonstrated a tendency for further metabolism into a glutathione (GSH) conjugate in rat hepatocytes, suggesting potential toxicity associated with reactive metabolite formation. The involvement of CYP-mediated bioactivation in this toxic pathway was further supported by irreversible inhibition using 1-aminobenzotriazole, a non-specific CYP inhibitor, which substantiated the role of CYP2D6 in the observed hepatotoxic effects.

Conclusion

In this study, metoprolol was characterized as a low-clearance compound based on its metabolic profile in plateable human hepatocytes. The plateable hepatocyte system demonstrated extensive metabolic capacity, with 22 metabolites of metoprolol identified for the first time. Functionally competent cytochrome P450 enzymes were maintained in human plateable hepatocytes, accurately recapitulating metabolite profiles generated by human recombinant CYP2D6 enzymes. The principal biotransformation pathways consisted of *O*-demethylation, mono-oxygenation and oxidative metabolism. Toxicologically, M10 was found to be metabolically converted into a glutathione (GSH) conjugate in rat plateable hepatocytes. The CYP-dependent nature of this hepatotoxic effect was confirmed through reversible inhibition using the non-specific CYP inhibitor 1-aminobenzotriazole. While weak hepatotoxicity occurred in rat hepatocytes at a supratherapeutic concentration of 500 µM, no significant hepatotoxicity was observed in human hepatocytes at metoprolol concentrations below 500 µM. Collectively, these findings validate plateable hepatocytes as a robust *in vitro* system for studying the metabolism of low-clearance compounds, offering valuable insights for preclinical drug safety assessment.

Supplementary material

Additional data are available at https://pub.iapchem.org/ojs/index.php/admet/article/view/2961, or from the corresponding author on request.

Human and Animal Rights: *All hepatocytes were purchased from commercially available vendors, there were no animal related experiments in this study.*

Funding: *None.*

Acknowledgements: *The author(s) thank the reviewers' valuable comments and suggestions.*

Conflict of interest: *The authors declare no conflict of interest, financial or otherwise.*

References

[1] N. Blanchard, N.J. Hewitt, P. Silber, H. Jones, P. Coassolo, T. Lave. Prediction of hepatic clearance using cryopreserved human hepatocytes: a comparison of serum and serum-free incubations. *Journal of Pharmacy and Pharmacology* **58** (2010) 633-641. http://doi.org/10.1211/jpp.58.5.0008

[2] Z. Zhou, M.J. Xu, B. Gao. Hepatocytes: A key cell type for innate immunity. *Cellular and Molecular Immunology* **13** (2016) 301-315. http://doi.org/10.1038/cmi.2015.97

[3] D. Dalvie, R. Scott Obach, P. Kang, C. Prakash, C.M. Loi, S. Hurst, A. Nedderman, L. Goulet, E. Smith, H.Z. Bu, D.A. Smith. Assessment of three human in vitro systems in the generation of major human excretory and circulating metabolites. *Chemical Research in Toxicology* **22** (2009) 357-368. http://doi.org/10.1021/tx8004357

[4] M.G. Soars, D.F. McGinnity, K. Grime, R.J. Riley. The pivotal role of hepatocytes in drug discovery. *Chemico-Biological Interactions* **168** (2007) 2-15. http://doi.org/10.1016/j.cbi.2006.11.002

[5] K.H. Grime, P. Barton, D.F. McGinnity. Application of in silico, in vitro and preclinical pharmacokinetic data for the effective and efficient prediction of human pharmacokinetics. *Molecular Pharmaceutics* **10** (2013) 1191-1206. http://doi.org/10.1021/mp300476z

[6] A.K. Sohlenius-Sternbeck, C. Jones, D. Ferguson, B.J. Middleton, D. Projean, E. Floby, J. Bylund, L. Afzelius. Practical use of the regression offset approach for the prediction of in vivo intrinsic clearance from hepatocytes. *Xenobiotica* **42** (2012) 841-852. http://doi.org/10.3109/00498254.2012.669080

[7] P. Chao, A.S. Uss, K. Cheng. Use of intrinsic clearance for prediction of human hepatic clearance. *Expert Opinion on Drug Metabolism and Toxicology* **6** (2010) 189-198. http://doi.org/10.1517/17425250903405622

[8] R.S. Obach. Predicting clearance in humans from in vitro data. *Current Topics in Medicinal Chemistry* **11** (2011) 334-339. http://doi.org/10.2174/156802611794480873

[9] E.L. Lecluyse, E. Alexandre. Isolation and culture of primary hepatocytes from resected human liver tissue. *Methods in Molecular Biology (Clifton, N.J.)* **640** (2010) 57-82. http://doi.org/10.1007/978-1-60761-688-7_3

[10] H.M. Jones, J.B. Houston. Substrate depletion approach for determining in vitro metabolic clearance: Time dependencies in hepatocyte and microsomal incubations. *Drug Metabolism and Disposition* **32** (2004) 973-982. http://doi.org/10.1124/dmd.104.000125

[11] A.P. Li, C. Lu, J.A. Brent, C. Pham, A. Fackett, C.E. Ruegg, P.M. Silber. Cryopreserved human hepatocytes: Characterization of drug-metabolizing activities and applications in higher throughput screening assays for hepatotoxicity, metabolic stability, and drug-drug interaction potential. *Chemico-Biological Interactions* **121** (1999) 17-35. http://doi.org/10.1016/S0009-2797(99)00088-5

[12] R. Murgasova. Further Assessment of the Relay Hepatocyte Assay for Determination of Intrinsic Clearance of Slowly Metabolised Compounds Using Radioactivity Monitoring and LC-MS Methods. *European Journal of Drug Metabolism and Pharmacokinetics* **44** (2019) 817-826. http://doi.org/10.1007/s13318-019-00571-x

[13] H.S. Brown, M. Griffin, J.B. Houston. Evaluation of cryopreserved human hepatocytes as an alternative in vitro system to microsomes for the prediction of metabolic clearance. *Drug Metabolism and Disposition* **35** (2007) 293-301. http://doi.org/10.1124/dmd.106.011569

[14] N.J. Hewitt, M.J.G. Lechón, J.B. Houston, D. Hallifax, H.S. Brown, P. Maurel, J.G. Kenna, L. Gustavsson, C. Lohmann, C. Skonberg, A. Guillouzo, G. Tuschl, A.P. Li, E. Lecluyse, G.M.M. Groothuis, J.G. Hengstler. Primary hepatocytes: Current understanding of the regulation of metabolic enzymes and transporter proteins, and pharmaceutical practice for the use of hepatocytes in metabolism, enzyme induction, transporter, clearance, and hepatotoxicity studies. *Drug Metabolism Reviews* **39** (2007) 159-234. http://doi.org/10.1080/03602530601093489

[15] A. Jetter, G.A. Kullak-Ublick. Drugs and hepatic transporters: A review. *Pharmacological Research* **154** (2020) 104234. http://doi.org/10.1016/j.phrs.2019.04.018

[16] R. Namdari, K. Jones, S.S. Chuang, S. Van Cruchten, Z. Dincer, N. Downes, L.F. Mikkelsen, J. Harding, S. Jäckel, B. Jacobsen, J. Kinyamu-Akunda, A. Lortie, S. Mhedhbi, S. Mohr, M.W. Schmitt, H. Prior. Species selection for nonclinical safety assessment of drug candidates: Examples of current industry practice. *Regulatory Toxicology and Pharmacology* **126** (2021) 105029. http://doi.org/10.1016/j.yrtph.2021.105029

[17] H. Prior, R. Haworth, B. Labram, R. Roberts, A. Wolfreys, F. Sewell. Justification for species selection for pharmaceutical toxicity studies. *Toxicology Research* **9** (2021) 758-770. http://doi.org/10.1093/TOXRES/TFAA081

[18] M. Darnell. T. Schreiter, K. Zeilinger, T. Urbaniak, T. Söderdahl, I. Rossberg, B. Dillnér, A.-L. Berg, J. C. Gerlach, T. B. Andersson. Cytochrome P450 induction in HepaRG cells cultured in a dynamic 3D bioreactor. *Drug Metabolism Reviews* **41** (2009) 1131-1138. http://doi.org/10.1124/dmd.110.037721

[19] S. Anthérieu, C. Chesné, R. Li, S. Camus, A. Lahoz, L. Picazo, M. Turpeinen, A. Tolonen, J. Uusitalo, C. Guguen-Guillouzo, A. Guillouzo. Stable expression, activity, and inducibility of cytochromes P450 in differentiated HepaRG cells. *Drug Metabolism and Disposition* **38** (2010) 516-525. http://doi.org/10.1124/dmd.109.030197

[20] B. Bonn, P. Svanberg, A. Janefeldt, I. Hultman, K. Grime. Determination of human hepatocyte intrinsic clearance for slowly metabolized compounds: Comparison of a primary hepatocyte/stromal cell co-culture with plated primary hepatocytes and hepaRG. *Drug Metabolism and Disposition* **44** (2016) 527-533. http://doi.org/10.1124/dmd.115.067769

[21] T.S. Chan, H. Yu, A. Moore, S.R. Khetani, D. Tweedie. Meeting the challenge of predicting hepatic clearance of compounds slowly metabolized by cytochrome P450 using a novel hepatocyte model, HepatoPac. *Drug Metabolism and Disposition* **41** (2013) 58-66. http://doi.org/10.1124/dmd.113.053397

[22] D. Ramsden, D.J. Tweedie, T.S. Chan, M.E. Taub, Y. Li. Bridging in vitro and in vivo metabolism and transport of faldaprevir in human using a novel cocultured human hepatocyte system, hepatopac. *Drug Metabolism and Disposition* **42** (2014) 394-406. http://doi.org/10.1124/dmd.113.055897

[23] D. Ramsden, D.J. Tweedie, R. St. George, L.Z. Chen, Y. Li. Generating an in vitro-in vivo correlation for metabolism and liver enrichment of a hepatitis C virus drug, faldaprevir, using a rat hepatocyte model (hepatopac). *Drug Metabolism and Disposition* **42** (2014) 407-414. http://doi.org/10.1124/dmd.113.055947

[24] L. Di, P. Trapa, R.S. Obach, K. Atkinson, Y.A. Bi, A.C. Wolford, B. Tan, T.S. McDonald, Y. Lai, L.M. Tremaine. A novel relay method for determining low-clearance values. *Drug Metabolism and Disposition* **40** (2012) 1960-1965. http://doi.org/10.1124/dmd.112.046425

[25] L. Di, R.S. Obach. Addressing the Challenges of Low Clearance in Drug Research. *AAPS Journal* **17** (2015) 352-357. http://doi.org/10.1208/s12248-014-9691-7

[26] K.A. Hoffmaster, R.Z. Turncliff, E.L. LeCluyse, R.B. Kim, P.J. Meier, K.L.R. Brouwer. P-glycoprotein expression, localization, and function in sandwich-cultured primary rat and human hepatocytes: Relevance to the hepatobiliary disposition of a model opioid peptide. *Pharmaceutical Research* **21** (2004) 1294-1302. http://doi.org/10.1023/B:PHAM.0000033018.97745.0d

[27] K. Kanda, R. Takahashi, T. Yoshikado, Y. Sugiyama. Total hepatocellular disposition profiling of rosuvastatin and pitavastatin in sandwich-cultured human hepatocytes. *Drug Metabolism and Pharmacokinetics* **33** (2018) 164-172. http://doi.org/10.1016/j.dmpk.2018.04.001

[28] B. Swift, N.D. Pfeifer, K.L.R. Brouwer. Sandwich-cultured hepatocytes: An in vitro model to evaluate hepatobiliary transporter-based drug interactions and hepatotoxicity. *Drug Metabolism Reviews* **42** (2010) 446-471. http://doi.org/10.3109/03602530903491881

[29] J.H. Brown, P. Das, M.D. DiVito, D. Ivancic, L.P. Tan, J.A. Wertheim. Nanofibrous PLGA electrospun scaffolds modified with type I collagen influence hepatocyte function and support viability in vitro. Acta *Biomaterialia* **73** (2018) 217-227. http://doi.org/10.1016/j.actbio.2018.02.009

[30] M. Oorts, J. Keemink, N. Deferm, R. Adriaensen, L. Richert, P. Augustijns, P. Annaert. Extra collagen overlay prolongs the differentiated phenotype in sandwich-cultured rat hepatocytes. *Journal of Pharmacological and Toxicological Methods* **90** (2018) 31-38. http://doi.org/10.1016/j.vascn.2017.10.007

[31] J. Keemink, M. Oorts, P. Annaert. Primary hepatocytes in sandwich culture. *Methods in Molecular Biology* **1250** (2014) 175-188. http://doi.org/10.1007/978-1-4939-2074-7_12

[32] P. Lancett, B. Williamson, P. Barton, R.J. Riley. Development and characterization of a human hepatocyte low intrinsic clearance assay for use in drug discovery. *Drug Metabolism and Disposition* **46** (2018) 1169-1178. http://doi.org/10.1124/dmd.118.081596

[33] N. Treijtel, A. Barendregt, A.P. Freidig, B.J. Blaauboer, J.C.H. Van Eijkeren. Modeling the in vitro intrinsic clearance of the slowly metabolized compound tolbutamide determined in sandwich-cultured rat hepatocytes. *Drug Metabolism and Disposition* **32** (2004) 884-891. http://doi.org/10.1124/dmd.32.8.884

[34] W. Xiao, G. Perry, K. Komori, Y. Sakai. New physiologically-relevant liver tissue model based on hierarchically cocultured primary rat hepatocytes with liver endothelial cells. *Integrative Biology (United Kingdom)* **7** (2015) 33-45. http://doi.org/10.1039/c5ib00170f

[35] R. Kostadinova, F. Boess, D. Applegate, L. Suter, T. Weiser, T. Singer, B. Naughton, A. Roth. A long-term three dimensional liver co-culture system for improved prediction of clinically relevant drug-induced hepatotoxicity. *Toxicology and Applied Pharmacology* **268** (2013) 1-16. http://doi.org/10.1016/j.taap.2013.01.012

[36] Y. Liu, J. Wei, J. Lu, D. Lei, S. Yan, X. Li. Micropatterned coculture of hepatocytes on electrospun fibers as a potential in vitro model for predictive drug metabolism. *Materials Science and Engineering C* **63** (2016) 474-484. http://doi.org/10.1016/j.msec.2016.03.025

[37] O. Ukairo, C. Kanchagar, A. Moore, J. Shi, J. Gaffney, S. Aoyama, K. Rose, S. Krzyzewski, J. Mcgeehan, M.E. Andersen, S.R. Khetani, E.L. Lecluyse. Long-term stability of primary rat hepatocytes in micropatterned cocultures. *Journal of Biochemical and Molecular Toxicology* **27** (2013) 204-212. http://doi.org/10.1002/jbt.21469

[38] Y. Liu, H. Li, S. Yan, J. Wei, X. Li. Hepatocyte cocultures with endothelial cells and fibroblasts on micropatterned fibrous mats to promote liver-specific functions and capillary formation capabilities. *Biomacromolecules* **15** (2014) 1044-1054. http://doi.org/10.1021/bm401926k

[39] S.R. Khetani, S.N. Bhatia. Microscale culture of human liver cells for drug development. *Nature Biotechnology* **26** (2008) 120-126. http://doi.org/10.1038/nbt1361

[40] S. March, V. Ramanan, K. Trehan, S. Ng, A. Galstian, N. Gural, M.A. Scull, A. Shlomai, M.M. Mota, H.E. Fleming, S.R. Khetani, C.M. Rice, S.N. Bhatia. Micropatterned coculture of primary human hepatocytes and supportive cells for the study of hepatotropic pathogens. *Nature Protocols* **10** (2015) 2027-2053. http://doi.org/10.1038/nprot.2015.128

[41] W.W.W. Wang, S.R. Khetani, S. Krzyzewski, D.B. Duignan, R.S. Obach. Accelerated communication assessment of a micropatterned hepatocyte coculture system to generate major human excretory and circulating drug metabolites. *Drug Metabolism and Disposition* **38** (2010) 1900-1905. http://doi.org/10.1124/dmd.110.034876

[42] J.M. Hutzler, B.J. Ring, S.R. Anderson. Low-turnover drug molecules: A current challenge for drug metabolism scientists. *Drug Metabolism and Disposition* **43** (2015) 1917-1928. http://doi.org/10.1124/dmd.115.066431

[43] P. Chao, T. Maguire, E. Novik, K.C. Cheng, M.L. Yarmush. Evaluation of a microfluidic based cell culture platform with primary human hepatocytes for the prediction of hepatic clearance in human. *Biochemical Pharmacology* **78** (2009) 625-632. http://doi.org/10.1016/j.bcp.2009.05.013

[44] E. Novik, T.J. Maguire, P. Chao, K.C. Cheng, M.L. Yarmush. A microfluidic hepatic coculture platform for cell-based drug metabolism studies. *Biochemical Pharmacology* **79** (2010) 1036-1044. http://doi.org/10.1016/j.bcp.2009.11.010

[45] I. Hultman, C. Vedin, A. Abrahamsson, S. Winiwarter, M. Darnell. Use of HμREL Human Coculture System for Prediction of Intrinsic Clearance and Metabolite Formation for Slowly Metabolized Compounds. *Molecular Pharmaceutics* **13** (2016) 2796-2807. http://doi.org/10.1021/acs.molpharmaceut.6b00396

[46] A. Dash, W. Inman, K. Hoffmaster, S. Sevidal, J. Kelly, R.S. Obach, L.G. Griffith, S.R. Tannenbaum. Liver tissue engineering in the evaluation of drug safety. *Expert Opinion on Drug Metabolism and Toxicology* **5** (2009) 1159-1174. http://doi.org/10.1517/17425250903160664

[47] A. Vivares, S. Salle-Lefort, C. Arabeyre-Fabre, R. Ngo, G. Penarier, M. Bremond, P. Moliner, J.F. Gallas, G. Fabre, S. Klieber. Morphological behaviour and metabolic capacity of cryopreserved human primary hepatocytes cultivated in a perfused multiwell device. *Xenobiotica* **45** (2015) 29-44. http://doi.org/10.3109/00498254.2014.944612

[48] C.M. Smith, C.K. Nolan, M.A. Edwards, J.B. Hatfield, T.W. Stewart, S.S. Ferguson, E.L. Lecluyse, J. Sahi. A comprehensive evaluation of metabolic activity and intrinsic clearance in suspensions and monolayer cultures of cryopreserved primary human hepatocytes. *Journal of Pharmaceutical Sciences* **101(10)** (2012) 3989-4002. http://doi.org/10.1002/jps.23262

[49] C.-C. Peng, U. Doshi, C. Prakash, A. Li. A Novel Plated Hepatocyte Relay Assay (PHRA) for In Vitro Evaluation of Hepatic Metabolic Clearance of Slowly Metabolized Compounds. *Drug Metabolism Letters* **10** (2016) 3-15. http://doi.org/10.2174/1872312809666150818111500

[50] J. Riede, B.M. Wollmann, E. Molden, M. Ingelman-Sundberg. Primary human hepatocyte spheroids as an in vitro tool for investigating drug compounds with low hepatic clearances. *Drug Metabolism and Disposition* **49** (2021) 501-508. http://doi.org/10.1124/dmd.120.000340

[51] E. Alexandre, A. Baze, C. Parmentier, C. Desbans, D. Pekthong, B. Gerin, C. Wack, P. Bachellier, B. Heyd, J.C. Weber, L. Richert. Plateable cryopreserved human hepatocytes for the assessment of cytochrome P450 inducibility: Experimental condition-related variables affecting their response to inducers. *Xenobiotica* **42** (2012) 968-979. http://doi.org/10.3109/00498254.2012.676693

[52] M. Darnell, M. Ulvestad, E. Ellis, L. Weidolf, T.B. Andersson. In vitro evaluation of major in vivo drug metabolic pathways using primary human hepatocytes and HepaRG cells in suspension and a dynamic three-dimensional bioreactor system. *Journal of Pharmacology and Experimental Therapeutics* **343** (2012) 134-144. http://doi.org/10.1124/jpet.112.195834

[53] S.J. Griffin, J.B. Houston. Prediction of in vitro intrinsic clearance from hepatocytes: Comparison of suspensions and monolayer cultures. *Drug Metabolism and Disposition* **33** (2005) 115-120. http://doi.org/10.1124/dmd.33.1.115

[54] N. Blanchard, E. Alexandre, C. Abadie, T. Lavé, B. Heyd, G. Mantion, D. Jaeck, L. Richert, P. Coassolo. Comparison of clearance predictions using primary cultures and suspensions of human hepatocytes. *Xenobiotica* **35** (2005) 1-15. http://doi.org/10.1080/00498250400021820

[55] EMA. Guideline on the investigation of drug interactions. *European Medicine Agency* **44** (2012) 1-59. https://www.ema.europa.eu/en/documents/scientific-guideline/guideline-investigation-drug-interactions-revision-1_en.pdf

[56] C.D. Thomas, S.A. Mosley, S. Kim, K. Lingineni, N. El Rouby, T.Y. Langaee, Y. Gong, D. Wang, S.O. Schmidt, P.F. Binkley, D.S. Estores, K. Feng, H. Kim, M. Kinjo, Z. Li, L. Fang, A.B. Chapman, R.M. Cooper-DeHoff, J.G. Gums, I.S. Hamadeh, L. Zhao, S. Schmidt, R.F. Frye, J.A. Johnson, L.H. Cavallari. Examination of Metoprolol Pharmacokinetics and Pharmacodynamics Across CYP2D6 Genotype-Derived Activity Scores. *CPT: Pharmacometrics and Systems Pharmacology* **9** (2020) 678-685. http://doi.org/10.1002/psp4.12563

[57] V.B. Boralli, E.B. Coelho, P.M. Cerqueira, V.L. Lanchote. Stereoselective analysis of metoprolol and its metabolites in rat plasma with application to oxidative metabolism. *Journal of Chromatography B: Analytical Technologies in the Biomedical and Life Sciences* **823** (2005) 195-202. http://doi.org/10.1016/j.jchromb.2005.06.038

[58] Laura Dean, Victoria M. Pratt, Stuart A. Scott, Munir Pirmohamed, Bernard Esquivel, Brandi L. Kattman, Adriana J. Malheiro. *Metoprolol Therapy and CYP2D6 Genotype*, Medical Genetics Summaries, Bethesda (MD): National Center for Biotechnology Information, US, 2012. https://pubmed.ncbi.nlm.nih.gov/28520381/

[59] S.-M. Huang, R. Temple, D.C. Throckmorton, L.J. Lesko. Drug interaction studies: study design, data analysis, and implications for dosing and labeling. *Clinical Pharmacology and Therapeutics* **81** (2007) 298-304. http://doi.org/10.1038/sj.clpt.6100054

[60] D.F. McGinnity, A.J. Parker, M. Soars, R.J. Riley. Automated definition of the enzymology of drug oxidation by the major human drug metabolizing cytochrome P450s. *Drug Metabolism and Disposition* **28** (2000) 1327-1334. https://doi.org/10.1016/S0090-9556(24)15081-7

[61] T. Yamamoto, H. Itoga, Y. Kohno, K. Nagata, Y. Yamazoe. Prediction of oral clearance from in vitro metabolic data using recombinant CYPs: Comparison among well-stirred, parallel-tube, distributed and dispersion models. *Xenobiotica* **35** (2005) 627-646. http://doi.org/10.1080/00498250500159371

[62] Y.R. Ma, Z. Rao, A.X. Shi, Y.F. Wang, J. Huang, M. Han, X.D. Wang, Y.W. Jin, G.Q. Zhang, Y. Zhou, F. Zhang, H.Y. Qin, X.A. Wu. Simultaneous determination of metformin, metoprolol and its metabolites in rat plasma by LC-MS-MS: Application to pharmacokinetic interaction study. *Journal of Chromatographic Science* **54** (2016) 1-9. http://doi.org/10.1093/chromsci/bmv097

[63] X. Li, G. Xing, X. Guo, Y. Wang, Z. Hu, M. Cheng, Y. Peng, J. Zheng. Identification of Metoprolol Tartrate-Derived Reactive Metabolites Possibly Correlated with Its Cytotoxicity. *Chemical Research in Toxicology* **35** (2022) 1059-1069. http://doi.org/10.1021/acs.chemrestox.2c00052

[64] B. Berger, F. Bachmann, U. Duthaler, S. Krähenbühl, M. Haschke. Cytochrome P450 enzymes involved in metoprolol metabolism and use of metoprolol as a CYP2D6 phenotyping probe drug. *Frontiers in Pharmacology* **9** (2018) 774. http://doi.org/10.3389/fphar.2018.00774

[65] P.M. Cerqueira, V.B. Boralli, E.B. Coelho, N.P. Lopes, L.F. Lopes Guimarães, P.S. Bonato, V.L. Lanchote. Enantioselective determination of metoprolol acidic metabolite in plasma and urine using liquid chromatography chiral columns: Applications to pharmacokinetics. *Journal of Chromatography B* **783** (2003) 433-441. http://doi.org/10.1016/S1570-0232(02)00705-5

[66] T. Xu, S. Bao, P. Geng, J. Luo, L. Yu, P. Pan, Y. Chen, G. Hu. Determination of metoprolol and its two metabolites in human plasma and urine by high performance liquid chromatography with fluorescence detection and its application in pharmacokinetics. *Journal of Chromatography B* **937** (2013) 60-66. http://doi.org/10.1016/j.jchromb.2013.08.017

[67] S.H. Bae, J.K. Lee, D.Y. Cho, S.K. Bae. Simultaneous determination of metoprolol and its metabolites, α-hydroxymetoprolol and O-desmethylmetoprolol, in human plasma by liquid chromatography with tandem mass spectrometry: Application to the pharmacokinetics of metoprolol associated with CYP2D6 genotypes. *Journal of Separation Science* **37** (2014) 1256-1264. http://doi.org/10.1002/jssc.201301353

[68] K.U. Seiler, K.J. Schuster, G.J. Meyer, W. Niedermayer, O. Wassermann. The Pharmacokinetics of Metoprolol and its Metabolites in Dialysis Patients. *Clinical Pharmacokinetics* **5** (1980) 192-198. http://doi.org/10.2165/00003088-198005020-00006

[69] J. Fang, H.A. Semple, J. Song. Determination of metoprolol, and its four metabolites in dog plasma. *Journal of Chromatography B* **809** (2004) 9-14. http://doi.org/10.1016/j.jchromb.2004.05.029

[70] K. Bachmann, J. Byers, R. Ghosh. Prediction of in vivo hepatic clearance from in vitro data using cryopreserved human hepatocytes. *Xenobiotica* **33** (2003) 475-483. http://doi.org/10.1080/0049825031000076177

[71] J. Brian Houston. Utility of in vitro drug metabolism data in predicting in vivo metabolic clearance. *Biochemical Pharmacology* **47** (1994) 1469-1479. http://doi.org/10.1016/0006-2952(94)90520-7

[72] B. Davies, T. Morris. Physiological parameters in laboratory animals and humans. *Pharmaceutical Research* **10** (1993) 1093-1095. http://doi.org/10.1023/A:1018943613122

[73] J. Louisse, M. Alewijn, A.A.C.M. Peijnenburg, N.H.P. Cnubben, M.B. Heringa, S. Coecke, A. Punt. Towards harmonization of test methods for in vitro hepatic clearance studies. *Toxicology in Vitro* **63** (2020) 104722. http://doi.org/10.1016/j.tiv.2019.104722

[74] S.J. Griffin, J.B. Houston. Comparison of fresh and cryopreserved rat hepatocyte suspensions for the prediction of in vitro intrinsic clearance. *Drug Metabolism and Disposition* **32** (2004) 552-558. http://doi.org/10.1124/dmd.32.5.552

[75] C. Quarterman, M. Kendall, D. Jack. The effect of age on the pharmacokinetics of metoprolol and its metabolites. *British Journal of Clinical Pharmacology* **11** (1981) 287-294. http://doi.org/10.1111/j.1365-2125.1981.tb00536.x

[76] R.M. Borkar, M.M. Bhandi, A.P. Dubey, V. Ganga Reddy, P. Komirishetty, P.P. Nandekar, A.T. Sangamwar, A. Kamal, S.K. Banerjee, R. Srinivas. An evaluation of the CYP2D6 and CYP3A4 inhibition potential of metoprolol metabolites and their contribution to drug-drug and drug-herb interaction by LC-ESI/MS/MS. *Biomedical Chromatography* **30** (2016) 1556-1572. http://doi.org/10.1002/bmc.3721

[77] B. Ma, R. Eisenhandler, Y. Kuo, P. Rearden, Y. Li, P.J. Manley, S. Smith, K. Menzel. Prediction of Metabolic Clearance for Low-Turnover Compounds Using Plated Hepatocytes with Enzyme Activity Correction. *European Journal of Drug Metabolism and Pharmacokinetics* **42** (2017) 319-326. http://doi.org/10.1007/s13318-016-0336-3